Integrative and Comparative Biology

Integrative and Comparative Biology, volume 55, number 2, pp. 217–227
doi:10.1093/icb/icv004

Society for Integrative and Comparative Biology

SYMPOSIUM

Capture of Prey, Feeding, and Functional Anatomy of the Jaws in Velvet Worms (Onychophora)

Georg Mayer,[1,*,†] Ivo S. Oliveira,[†] Alexander Baer,[†] Jörg U. Hammel,[‡] James Gallant[§] and Rick Hochberg[§]

*Department of Zoology, Institute of Biology, University of Kassel, Heinrich-Plett-Str. 40, D-34132 Kassel, Germany; [†]Animal Evolution and Development, Institute of Biology, University of Leipzig, D-04103 Leipzig, Germany; [‡]Institute of Materials Research, Helmholtz-Zentrum Geesthacht, Outstation at DESY, Building 25c Notkestr. 85, D-22607 Hamburg, Germany; [§]Department of Biology, University of Massachusetts Lowell, Lowell, MA 01854, USA

From the symposium "Soft Bodies, Hard Jaws: Phylogenetic Diversity of Prey Capture and Processing in Jawed, Soft-bodied Invertebrates" presented at the annual meeting of the Society for Integrative and Comparative Biology, January 3–7, 2015 at West Palm Beach, Florida.

[1]E-mail: gmayer@onychophora.com

Synopsis Onychophorans are carnivorous, terrestrial invertebrates that occur in tropical and temperate forests of the Southern Hemisphere and around the Equator. Together with tardigrades, onychophorans are regarded as one of the closest relatives of arthropods. One of the most peculiar features of onychophorans is their hunting and feeding behavior. These animals secrete a sticky slime, which is ejected via a pair of slime-papillae, to entangle the prey. After the prey has been immobilized, its cuticle is punctured using a pair of jaws located within the mouth. These jaws constitute internalized appendages of the second body segment and are innervated by the deutocerebrum; thus, they are homologous to the chelicerae of chelicerates, and to the (first) antennae of myriapods, crustaceans, and insects. The jaws are also serial homologs of the paired claws associated with each walking limb of the trunk. The structure of the jaws is similar in representatives of the two major onychophoran subgroups, the Peripatidae and Peripatopsidae. Each jaw is characterized by an outer and an inner blade; while the outer blade consists only of a large principal tooth and up to three accessory teeth, the inner blade bears numerous additional denticles. These denticles are separated from the remaining part of the inner jaw by a diastema and a soft membrane only in peripatids. The onychophoran jaws are associated with large apodemes and specialized muscles that enable their movement. In contrast to the mandibles of arthropods, the onychophoran jaws are moved along, rather than perpendicular to, the main axis of the body. Our elemental analysis reveals an increased incorporation of calcium at the tip of each blade, which might provide rigidity, whereas there is no evidence for incorporation of metal or prominent mineralization. Stability of the jaw might be further facilitated by the cone-in-cone organization of its cuticle, as each blade consists of several stacked, cuticular elements. In this work, we summarize current knowledge on the jaws of onychophorans, which are a characteristic feature of these animals.

Introduction

Onychophorans or velvet worms (Fig. 1A) are soft-bodied, terrestrial invertebrates that inhabit decaying logs and leaf litter of tropical and temperate forests in the Southern Hemisphere and around the Equator (Mayer 2007, 2015; Oliveira et al. 2012b). The approximately 200 described species of Onychophora are classified in two major subgroups: the Peripatidae and Peripatopsidae, which most likely diverged 380–300 million years ago, i.e., before the breakup of Gondwana (Allwood et al. 2010; Braband et al. 2010; Mayer 2007; Mayer and Oliveira 2013; Murienne et al. 2014). The anatomy of velvet worms has changed little since the divergence of the two subgroups and representatives of Peripatidae and Peripatopsidae notably display a similar anatomy (Ruhberg and Mayer 2013).

The onychophoran trunk exhibits 13–43 pairs of walking limbs, each equipped with a pair of sclerotized claws, hence the name Onychophora or "clawbearers" for the entire clade (Oliveira and Mayer

Advanced Access publication March 30, 2015

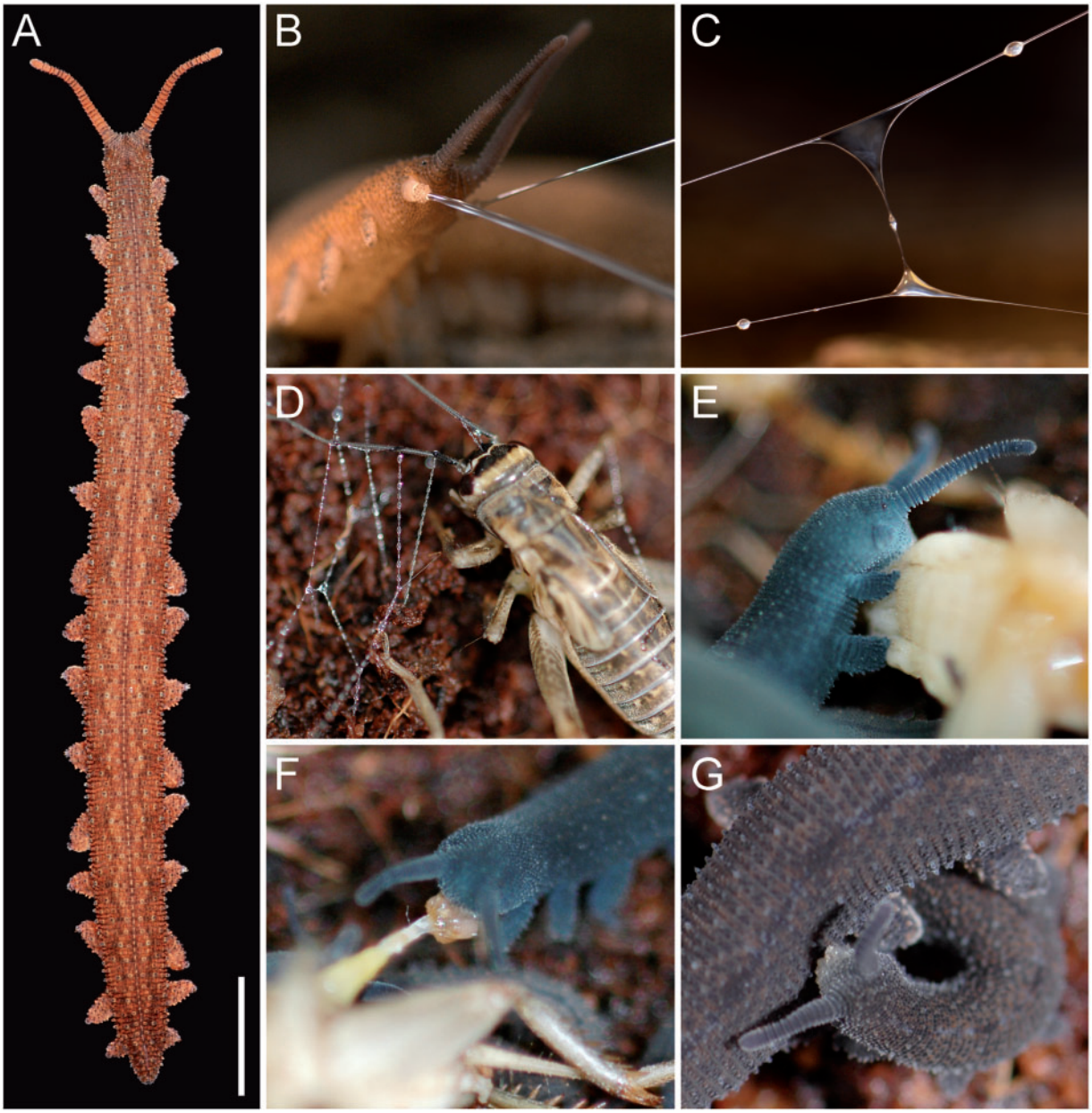

Fig. 1 Habitus, capture of prey, and feeding and biting behaviors of onychophorans. (**A**) Walking individual of the peripatopsid *Ooperipatus hispidus*. (**B**) Anterior end of a peripatid (*Principapillatus hitoyensis*) caught in the act of ejecting slime. (**C**) Detail of the ejected slime of *P. hitoyensis*. (**D**) Cricket (*Acheta domestica*) entangled by threads of slime. (**E**) A peripatopsid (*Euperipatoides rowelli*) feeding on a cricket. (**F**) An individual of *E. rowelli* trying to drag away a piece of a cricket. (**G**) A peripatopsid (*Phallocephale tallagandensis*) biting another specimen of the same species.

2013; Ruhberg and Mayer 2013). The three anteriormost pairs of limbs have been modified into specialized cephalic appendages, including antennae, jaws, and slime-papillae (Figs. 1A and 2A, B; Eriksson and Budd 2000; Eriksson et al. 2003; Mayer et al. 2010; Martin and Mayer 2014). While the antennae and the slime-papillae do not have any sclerotized parts, each onychophoran jaw bears heavily sclerotized outer and inner jaw blades (Oliveira and Mayer 2013). The name "mandibles" has been commonly applied to the onychophoran jaws (e.g., Bouvier 1905; Henry 1948; Ruhberg 1985), but this pair of appendages is clearly not homologous to the mandibles of arthropods, as it belongs to the second, rather than to the fourth body segment (Eriksson et al. 2003, 2010; Mayer et al. 2010; Whitington and Mayer 2011; Ou et al. 2012; Martin and Mayer 2014).

Like other representatives of Ecdysozoa (=molting animals), onychophorans molt their chitinous cuticle periodically by a process governed by the ecdysteroid hormones (Manton 1938; Holliday 1942; Hackman and Goldberg 1975; Campiglia and Lavallard 1989, 1990; Hoffmann 1997). Within the Ecdysozoa, Onychophora is commonly united with Tardigrada and Arthropoda in the clade Panarthropoda, although the exact relationship among these three animal groups remains unresolved (Mayer and Whitington 2009a; Rota-Stabelli et al. 2010; Campbell et al. 2011; Nielsen 2012; Mayer et al. 2013a, 2013b). In contrast to their relatives, the arthropods and tardigrades, the overall anatomy of the onychophoran body has remained largely unchanged since the Early Cambrian and extant onychophorans strikingly resemble the habitus of fossil lobopodians, a non-monophyletic assemblage of stem-group representatives of Panarthropoda, Onychophora, Tardigrada, and/or Arthropoda (e.g., Maas et al. 2007; Ma et al. 2009; Liu et al. 2011; Haug et al. 2012; Ou et al. 2012; Smith and Ortega-Hernández 2014). Herein we provide an outline of our current knowledge about the feeding mechanisms, functional morphology, and elementary composition of the jaws in Onychophora.

Materials and methods

Specimens

Four species of Peripatidae from Costa Rica and Brazil and five species of Peripatopsidae from Chile and Australia were studied (Table 1). Specimens were collected and maintained in the laboratory as described previously (Mayer 2007; Baer and Mayer 2012; Oliveira et al. 2012a; Oliveira and Mayer 2013). All animal treatments complied with the Principles of Laboratory Animal Care and the German Law on the Protection of Animals.

Scanning electron microscopy

Specimens were fixed in 4% formaldehyde or preserved in 70% ethanol and then processed as described previously (Mayer 2007). After dehydration in an ethanol series, specimens were dried in a CPD 030 Critical-Point Dryer (BAL-TEC AG, Balzers, Liechtenstein), coated with gold in a SCD 040 Sputter Coater (BALZERS UNION, Balzers, Liechtenstein), and examined in a Quanta 200 Scanning Electron Microscope (FEI, Hillsboro, OR, USA). Jaws were dissected from specimens preserved in 70% ethanol, rinsed in distilled water for 30 min, and digested overnight in a solution of 10% pepsin (0.3 g pepsin in 3 mL distilled water with two drops of 2M HCl) to remove excess tissue and processed further for scanning electron microscopy (SEM).

Synchrotron radiation-based X-ray micro-computer tomography

Specimens were fixed overnight in 4% paraformaldehyde in phosphate-buffered saline (PBS; 0.1M, pH 7.4). After several washes in PBS, specimens were postfixed in 1% osmium tetroxide in PBS, dehydrated in an ethanol series, dried in a critical-point dryer (CPD 030, BAL-TEC AG, Balzers, Liechtenstein) and mounted onto standardized sample holders (Helmholtz-Zentrum Geesthacht) for synchrotron radiation-based X-ray micro-computer tomography. The samples were imaged by synchrotron radiation-based X-ray microtomography operated by Helmholtz-Zentrum-Geesthacht at beamline P05 (Haibel et al. 2010; Greving et al. 2014) of the storage-ring PETRA III at Deutsches Elektronen Synchrotron (DESY, Hamburg, Germany) at 15 KeV in the attenuation contrast mode. We recorded 900 equally spaced projections between 0 and π. For tomographic reconstruction of the 3D datasets, the algorithm "back projection of filtered projections" (Huesman et al. 1977) was used to yield 32-bit floating-point image-stacks with isotropic voxel size of $(1.28\,\mu m)^3$. Segmentation of jaws was performed manually by labeling the structures in AVIZO 8.1 (FEI Visualization Sciences Group, Burlington, MA, USA). We obtained separate image-stacks for the left and right jaws, as well as for the head, based on the jaws' label-fields using the open-source software FIJI (Schindelin et al. 2012) and applying mask-image filters for further visualization and the volume rendering in VG Studio MAX 2.2 (Volume Graphics, Heidelberg, Germany).

Transmission electron microscopy

Specimens were fixed overnight in 2.5% glutaraldehyde in 0.1M sodium cacodylate, pH 7.0. After several washes in 0.1M sodium cacodylate, specimens were postfixed in 0.2% osmium tetroxide in 0.1M sodium cacodylate, dehydrated in an acetone series, and embedded in Araldite (Huntsman Advanced Materials, Basel, Switzerland) as described previously (Mayer et al. 2005; Mayer 2006). Specimens were then cut with a diamond knife into series of silver interference-colored (55–65 nm) sections on an ultramicrotome (Reichert Jung 2050 SuperCut, Leica Microsystems, Wetzlar, Germany). The sections were mounted on Formvar-coated, single-slot copper grids, automatically stained with uranyl acetate and lead citrate in an ultrostainer (Nanofilm

Table 1 The onychophoran species studied and their corresponding locality data

Peripatidae	
Epiperipatus acacioi Marcus and Marcus, 1955	Estação Ecológica do Tripuí, 20°23′S, 43°34′W, 1215 m, Ouro Preto, Minas Gerais, Brazil
Epiperipatus biolleyi Bouvier, 1902	Los Juncos, 83°57′W, 10°00′N, 1750–1800 m, Cascajal de Coronado, near San José, Costa Rica
Principapillatus hitoyensis Oliveira et al., 2012	Reserva Biológica Hitoy Cerere, 09°40′N, 83°02′W, 300 m, Province of Limón, region of Talamanca, Costa Rica
gen. et sp. (undescribed species)	Parque Ambiental do Utinga, 01°24′S, 48°24′W, 38 m, Belém, Pará, Brazil
Peripatopsidae	
Euperipatoides rowelli Reid, 1996	Tallaganda State Forest, 35°26′S, 149°33′E, 954 m, New South Wales, Australia
Metaperipatus blainvillei Gervais, 1837	Forest near Lago Tinquilco, 39°09′S, 71°42′W, 815 m, IX Region de la Araucania, Chile
Metaperipatus inae Mayer, 2007	forest near Contulmo, 38°01′S, 73°11′W, 390 m, VIII Region del Biobio, Chile
Ooperipatus hispidus Reid, 1996	Tallaganda State Forest, 35°26′S, 149°33′E, 954 m, New South Wales, Australia
Phallocephale tallagandensis Reid, 1996	Tallaganda State Forest, 35°26′S, 149°33′E, 954 m, New South Wales, Australia

TEM Stainer, Nanofilm Technologies GmbH, Göttingen, Germany), and imaged in a transmission electron microscope (CM 120, Philips/FEI).

Semi-thin sectioning and light microscopy

For semi-thin sectioning, specimens were embedded in Araldite as described for transmission electron microscopy and cut with a diamond knife into series of sections 0.5–1.0 μm thick on an ultramicrotome (Reichert Jung 2050 SuperCut, Leica Microsystems). The semi-thin sections were then placed on glass slides and stained with Toluidine Blue (Mayer and Tait 2009). The sections were analyzed with a light microscope (Leica Leitz DMR), equipped with a digital camera (PCO AG SensiCam, Kelheim, Germany).

Phalloidin-rhodamine staining and confocal laser-scanning microscopy

Heads of embryos at an advanced developmental stage were fixed overnight in 4% paraformaldehyde in 0.1M PBS, pH 7.4, at room temperature. They were then rinsed in several changes of PBS and incubated for 1 h in a solution containing phalloidin-rhodamine (Molecular Probes, currently Invitrogen, Carlsbad, CA, USA; catalogue no. R-415300; to the 300 U stock, 1.5 mL methanol was added, and 10 μL aliquots were stored at −20°C; prior to use, methanol was dried and 200 μL PBS were added to each aliquot) (see Mayer and Whitington [2009a, 2009b] for further details). After several rinses in PBS, the specimens were mounted on glass slides in Vectashield Mounting Medium (Vector Laboratories Inc., Burlingame, CA, USA; catalogue no. H-1000). They were analyzed with the confocal laser-scanning microscope LSM 510 META (Carl Zeiss MicroImaging GmbH, Jena, Germany). The image stacks were merged into final projections with the Zeiss LSM IMAGE BROWSER software (v. 4.0.0.241).

Energy-dispersive X-ray spectroscopy

Jaws were dissected from molted skins and prepared for SEM as described above, except that they were not treated with pepsin/HCl solution. Prior to examination, the jaws were mounted on an aluminum SEM stub and coated with gold-palladium using a Denton Vacuum Desk IV (Denton Vacuum, LLC, Moorestown, NJ, USA). Energy dispersive X-ray spectroscopy (EDS) spectra were collected with a JEOL 7410-140F Field Emission Scanning Electron Microscope (FE-SEM; JEOL, Inc., Peabody, MA, USA) with an energy dispersive spectrometer. Spectra were analyzed with EDAX Genesis version 4.61 (EDAX Inc., Mahwah, NJ, USA). Spectra were collected for 100 s at 10 mm working distance, an accelerating voltage of 20 kV, emission current of 10 μA, and probe current of 15.

Photography and processing of the final images

Photographs of living animals and slime were taken with a Nikon D70s SLR camera (Nikon Corporation, Tochigi, Japan). Optimal-quality light micrographs were achieved by using the AnalySIS software package (''Extended Focal Imaging'' and ''Multiple Image Alignment'' functions) and Photoshop CS4 (Adobe, San Jose, CA, USA). Final panels were designed with Illustrator CS4 (Adobe) and exported in the Tagged Image File Format.

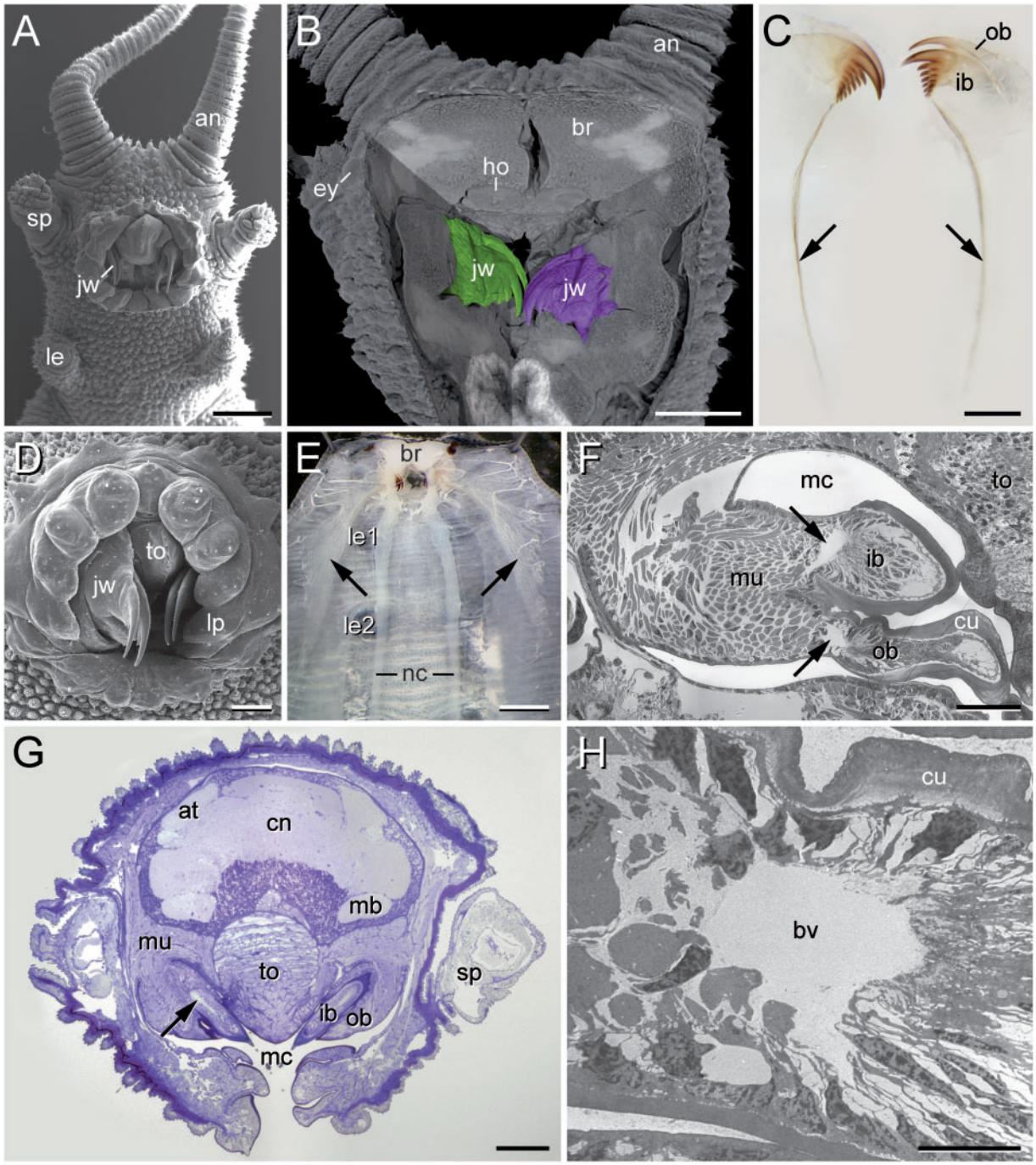

Fig. 2 Position and anatomy of onychophoran jaws and associated structures. (**A**) Scanning electron micrograph of the anterior end of *Metaperipatus inae* showing the three paired, modified, cephalic appendages: antennae, jaws, and slime-papillae. (**B**) Volume rendering of the head of *Euperipatoides rowelli* based on X-ray microtomography data illustrating the position of the jaws (artificially colored in green and purple) within the head. (**C**) Light micrograph of molted jaws of *M. inae*. Arrows point to the associated apodemes. (**D**) Scanning electron micrograph of the mouth of an undescribed peripatid species from Brazil showing extended jaws. (**E**) Stereomicrograph of a dissected specimen of *E. rowelli* demonstrating the extent and attachment sites of musculature associated with the apodemes (arrows). Numerous white, fiber-like structures are the tracheal tubes filled with air. (**F**) Transmission electron micrograph of jaws of a late-stage embryo of *Epiperipatus biolleyi*. Arrows point to the developing blood vessels at the basis of each jaw-blade. (**G**) Light micrograph of a cross-sectioned head of *Metaperipatus blainvillei* at the level of jaws (semi-thin section stained with Toluidine blue). Arrow points to a blood vessel within the jaw. (**H**) Detail of the blood vessel in the same specimen of *E. biolleyi* as in F. Abbreviations: an, antenna; at, antennal tract; br, brain; bv, blood vessel; cn, central brain neuropile; cu, cuticle; ey, eye; ho, hypocerebral organ; ib, inner jaw blade; jw, jaw; le, leg; le1, le 2, position of first and second legs; lp, lip papilla; mb, mushroom body; mc, mouth cavity; mu, jaw musculature; nc, nerve cords; ob, outer jaw blade; sp, slime papilla; to, tongue. Scale bars = 500 μm (A), 200 μm (B–D, G), 1 mm (E), 50 μm (F), 10 μm (H). (This figure is available in black and white in print and in color at *Integrative and Comparative Biology* online.)

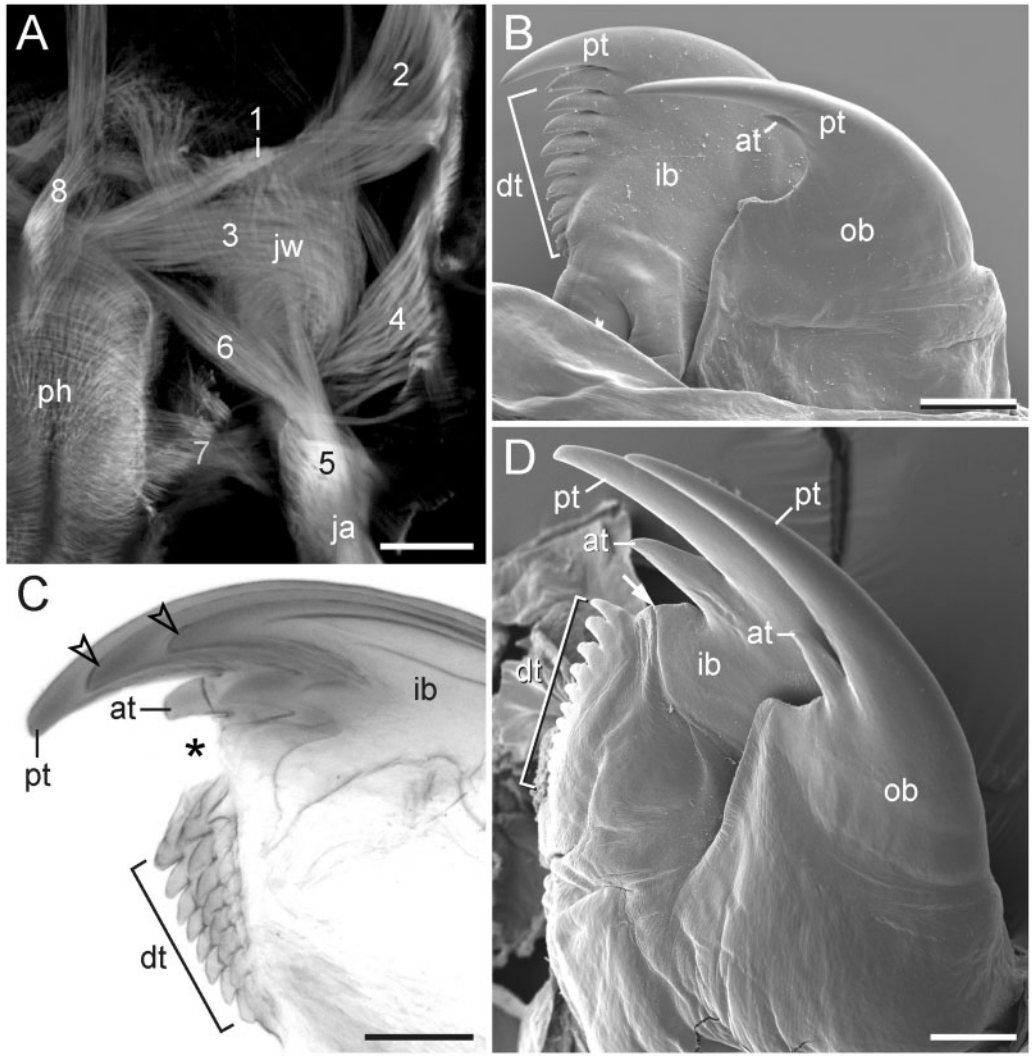

Fig. 3 The structure of onychophoran jaws. (**A**) Musculature associated with the jaw and its apodeme in *Principapillatus hitoyensis* (Peripatidae). Phalloidin-rhodamine staining. Projection of confocal z-series. Note the complex arrangement of muscles, which are numbered according to Oliveira and Mayer (2013). (**B**) Scanning electron micrograph of the outer and inner jaw-blades of the peripatopsid *Metaperipatus inae*. (**C**) Light micrograph of the inner jaw-blade of the peripatid *Epiperipatus acacioi*, demonstrating the cone-in-cone arrangement of cuticular elements (arrowheads). Asterisk demarcates the diastema. (**D**) Scanning electron micrograph of the outer and inner jaw-blades of the peripatid *Principapillatus hitoyensis*. Arrow points to the soft diastemal membrane. Abbreviations: at, accessory tooth; dt, denticles; ib, inner blade; ja, jaw apodeme muscle; jw, position of jaw; ob, outer blade; ph, pharynx; pt, primary tooth. Scale bars = 100 μm (A–D).

Results and discussion

Prey-capture and feeding behavior of onychophorans

One of the most peculiar features of onychophorans is their hunting and feeding behavior, as these animals use a sticky slime for capturing prey and for defense (Fig. 1B–D; Manton and Heatley 1937; Lavallard and Campiglia 1971; Ruhberg and Storch 1977; Read and Hughes 1987; Baer and Mayer 2012). The slime is produced and stored in large glands, the structure of which differs between representatives of Peripatidae and Peripatopsidae. While the glandular endpieces are distributed along the duct of the slime gland in peripatopsids, they are condensed in numerous repeated rosettes in peripatids (Baer and Mayer 2012).

Once the potential prey has been localized using the sensory antennae, the glue-like slime is ejected via the slime-papillae and entangles the target (Fig. 1B–D), e.g., crickets, amphipods, woodlice, and other soil-dwelling arthropods (Manton and Heatley 1937; Ruhberg 1985; Read and Hughes 1987; Baer and Mayer 2012). The mouth is then pressed against the body of the immobilized prey (Fig. 1E), whose cuticle is punctured using the

jaws, and the prey is injected with digestive saliva (Manton and Heatley 1937; Ruhberg 1985; Baer and Mayer 2012). The extra-intestinally predigested and liquefied contents are then ingested using a sucking pharynx (Mayer et al. 2013a; Nielsen 2013). Occasionally, large pieces are also torn off the prey and swallowed (Fig. 1F). After feeding, the undigested remains are enclosed in a peritrophic membrane and egested within 18 h after the commencement of feeding (Manton and Heatley 1937; de Mets et al. 1964; Ruhberg 1985). The onychophoran jaws are not only used for puncturing the prey's cuticle but also for biting rivals—a behavior that occurs frequently in captivity (Fig. 1G; Reinhard and Rowell 2005).

Functional anatomy of onychophoran jaws

Similar to the limbs of the trunk, the jaws arise from the lateral/ventrolateral regions of the body early in development, but they are incorporated into the definitive cavity of the mouth during ontogeny (Kennel 1885; Ou et al. 2012; Martin and Mayer 2014). In adult onychophorans, the jaws are located on either side of the tongue within the mouth (Fig. 2A, D, G). The tongue and the lip papillae surrounding the mouth fit closely against the jaw base, which helps to maintain the suction while feeding (Manton and Heatley 1937). The onychophoran jaws are tilted at about 45° toward the midline (Fig. 2B, G; Supplementary Movie S1) and, in contrast to the arthropods' mandibles, they are moved along, rather than perpendicular to, the main axis of the body (Manton and Heatley 1937; Ruhberg 1985; Ruhberg and Mayer 2013).

Each jaw is composed of an inner and outer blade and associated with a long, hollow, sclerotized posterior apodeme (arrows in Fig. 2C). The apodemes and the cuticle covering the jaws are molted periodically, together with the remaining cuticle of the body (Manton 1938; Holliday 1942; Oliveira and Mayer 2013). The molted jaws and their apodemes appear darker than the remaining cuticle, indicating a melanization or a higher degree of sclerotization of these structures compared with the rest of the body (Fig. 2C). Each jaw is associated with prominent intrinsic and extrinsic musculature, which shows a complex arrangement and is richly supplied with tracheal tubes (Figs. 2E–G and 3A) (Oliveira and Mayer 2013). The most prominent muscles are those associated with the jaws' apodemes. These muscles attach each apodeme to the dorsolateral body wall and extend as far behind as the region posterior to the second pair of legs (arrows in Fig. 2E). At the base of each jaw, there are hollow spaces that appear to be blood vessels (Fig. 2F–H). These blood vessels may be part of the hydrostatic skeleton of the onychophoran body and act as fluid-filled antagonists to the jaw's musculature.

Table 2 Values obtained from the elemental analysis of jaw-blades in the onychophoran *Euperipatoides rowelli* using energy-dispersive X-ray spectroscopy

Location[a]	C	N	O	Mg	S	Ca
Body	62.46	10.21	25.87	0.22	0.66	0.58
Distal-1	58.33	8.76	30.48	0.23	0.17	2.03
Distal-2	72.42	5.42	19.96	0.10	0.22	1.87
Distal-3	62.13	7.62	25.55	0.20	0.31	4.18
Mid-1	57.34	9.34	31.54	0.14	0.17	1.47
Mid-2	59.53	8.61	28.84	0.26	0.34	2.42
Mid-3	62.23	7.29	28.01	0.13	0.34	1.99
Proximal-1	60.92	9.06	27.83	0.23	0.43	1.54
Proximal-2	60.11	8.23	29.33	0.08	0.34	1.91
Proximal-3	60.52	7.97	29.28	0.17	0.27	1.79

Note: Values are in weight as a percentage of the total area scanned. [a]Three samples per location in the blade were analyzed (numbered 1–3).

The structure of the jaws is similar, albeit not the same, in representatives of Peripatidae and Peripatopsidae (Fig. 3B–D). The distal portion of each jaw is equipped with a pair of blades: an outer and an inner blade. In both peripatids and peripatopsids, the outer blade appears claw-like and consists of a large principal tooth and one to three smaller accessory teeth (Fig. 3B, D). In contrast, the structure of the inner blade clearly differs between Peripatidae and Peripatopsidae. While the principal tooth is associated with numerous denticles, forming a unitary blade in representatives of Peripatopsidae (Fig. 3B), the principal tooth that may be associated with one to three accessory teeth is separated from the blade of the denticle by a diastema and a soft diastemal membrane in representatives of Peripatidae (Fig. 3C, D). This membrane may act as a joint-like structure, allowing the denticle's blade to move independently from the remaining portion of the jaw (Oliveira and Mayer 2013).

In both Peripatidae and Peripatopsidae, each blade of the jaw consists of several stacked, cuticular elements (Fig. 3C) (e.g., Oliveira et al. 2010, 2011; Smith and Ortega-Hernández 2014). While the outer element is shed during each molt, the inner layer of epidermal cells continuously produces additional elements inside the blade of the jaw. The cone-in-cone arrangement of cuticular elements is

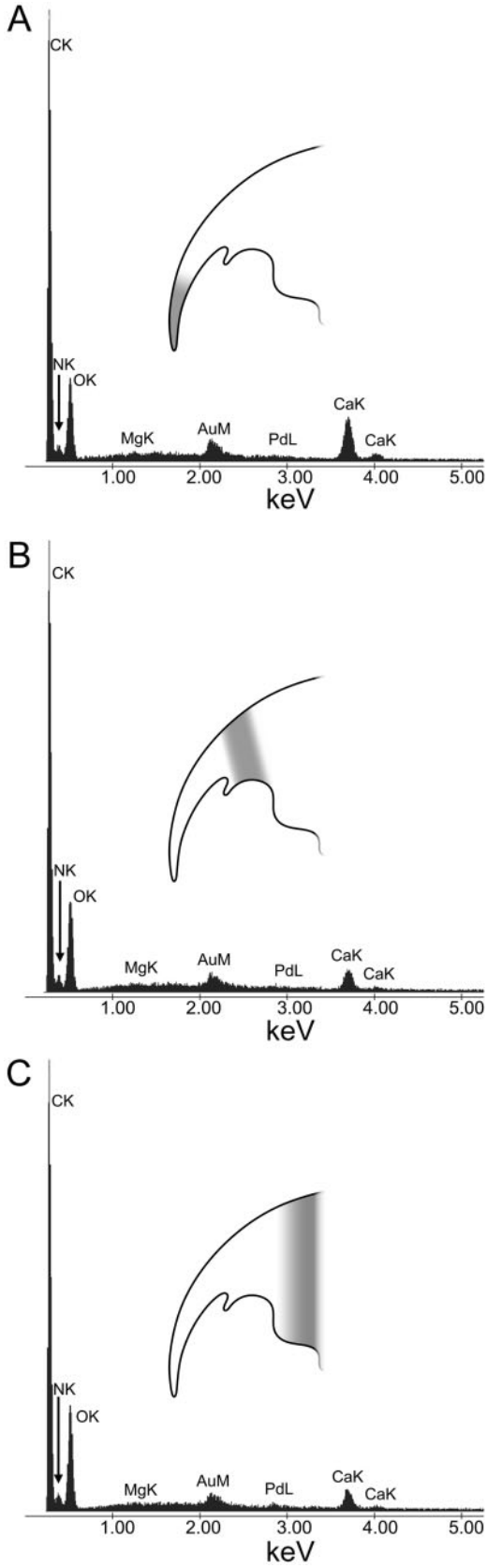

Fig. 4 Elemental histograms of the blades of the jaw in the onychophoran *Euperipatoides rowelli* using energy-dispersive X-ray spectroscopy. (**A**) Distal region. (**B**) Mid region. (**C**) Proximal region. Note that the tip of the blade contains more calcium than the remaining regions. The high content of carbon and oxygen is most likely due to the mainly chitinous composition of jaw-blades (see also Table 2 for relative amounts of nitrogen). The labels K and M refer to the K-shell and M-shell X-ray peaks. Peaks that cannot be resolved in the figure (e.g., silicon) had their atomic labels removed for clarity (see Table 2). Gold (Au) and palladium (Pd) are present here as minor peaks from sputter coating with a gold-palladium alloy; these atoms are not included in the quantitative analysis (Table 2).

not restricted to the jaws but has also been reported for the claws of the onychophoran foot (Smith and Ortega-Hernández 2014), and it is likely that these stacked elements add stability to these sclerotized structures. Hence, there are several correspondences between the onychophoran jaws and claws, as they share an overall sickle-like shape, a cone-in-cone arrangement of their cuticle, apodemes associated with extrinsic musculature, and they are the only sclerotized structures of the onychophoran body. These specific correspondences support serial homology of the onychophoran claws and jaws, suggesting that the jaws evolved from the distal portions of the corresponding limbs in the last common ancestor of Onychophora (Manton and Heatley 1937; Oliveira and Mayer 2013).

Analyses of energy-dispersive X-ray spectroscopy in the peripatopsid *Euperipatoides rowelli* show minimal variation in composition between the different regions of the blade of the jaws (Fig. 4A–C; Table 2). There is a high content of carbon, nitrogen, and oxygen in all parts of the blade (Table 2), likely due to the presence of α-chitin and the various proteins to which it may bind (Lotmar and Picken 1950; Rudall 1955). In addition to these expected elements, there is a mostly uniform layer of calcium across the entire blade. However, there is a slight increase in the total calcium content along the proximal–distal axis of the blade (Fig. 4A–C; Table 2). While the distal and mid scans of the blade vary only slightly, the proximal scans also have sulfur at higher levels than the distal scans, although still at minimal levels (<0.5 wt%; Table 2). This sulfur may be due to a higher concentration of disulfide bonds in this area (Subramoniam and Azariah 1974) than in more distal regions, as such bonds are believed to play a role in the folding and stability of proteins secreted to the extracellular medium (Sevier and Kaiser 2002). Since the onychophoran cuticle is generally rich in such extracellular proteins (Krishnan 1970; Subramoniam and Azariah 1974; Hackman and

Goldberg 1975), this finding suggests that there may be more protein and less calcium at the base and more calcium and less protein at the tip of the jaw. The increased incorporation of calcium at the tip of the blade might provide the additional rigidity required for efficient functioning of the onychophoran jaws, e.g., puncturing the cuticle or exoskeleton of their prey. Notably, our elemental analysis provides no evidence for incorporation of metal or prominent mineralization beyond the assimilation of calcium into the jaws of onychophorans; this differs from the elemental composition of arthropods' mandibles (Schofield et al. 2003; Cribb et al. 2009). However, encrustations of calcium carbonate have been reported from stylets of tardigrades (Guidetti et al. 2012) and these might be derivatives of claws of a modified pair of cephalic appendages (Halberg et al. 2009; Ou et al. 2012; Mayer et al. 2013a).

Conclusions

A recent experimental study revealed that the onychophoran claws and jaws are highly resistant to decay (Murdock et al. 2014). We have shown herein that the incorporation of calcium and probably also phenols and chinons (=sclerotization) rather than an impregnation with metals might be one of the reasons for the stability of onychophorans' jaw-blades. Despite their resistance to decay, no comparable structures have been identified in the corresponding body segment of any fossil lobopodians so far, although claws are known from various taxa (e.g., Hou and Bergström 1995; Hou et al. 2004; Ma et al. 2009; Ou et al. 2012; Liu and Dunlop 2014; Smith and Ortega-Hernández 2014). This supports the hypothesis that the jaws are a derived feature (=autapomorphy) of Onychophora (Ruhberg and Mayer 2013). Hence, the jaws must have evolved in the onychophoran lineage prior to the divergence of Peripatidae and Peripatopsidae approximately 380 million years ago (Murienne et al. 2014). Comparative anatomy of onychophorans' jaws suggests that these structures most likely evolved from the distal portions of an ancestral pair of walking limbs and that their blades are derivatives of the claws of these appendages (Oliveira and Mayer 2013).

Acknowledgments

The authors are thankful to the members of the Mayer laboratory for taking care of the animals.

Funding

This work was supported by the Conselho Nacional de Desenvolvimento Científico e Tecnológico [CNPq: 290029/2010-4 to I.S.O.]; the Doktorandenförderplatz of the University of Leipzig [DFPL: U00022 to A.B.]; and the Emmy Noether Programme of the German Research Foundation [DFG: Ma 4147/3-1 to G.M.].

Supplementary data

Supplementary data available at *ICB* online.

References

Allwood J, Gleeson D, Mayer G, Daniels S, Beggs JR, Buckley TR. 2010. Support for vicariant origins of the New Zealand Onychophora. J Biogeogr 37:669–81.

Baer A, Mayer G. 2012. Comparative anatomy of slime glands in Onychophora (velvet worms). J Morphol 273:1079–88.

Bouvier EL. 1905. Monographie des Onychophores. Ann Sci Nat Zool Biol Anim 2:1–383.

Braband A, Podsiadlowski L, Cameron SL, Daniels S, Mayer G. 2010. Extensive duplication events account for multiple control regions and pseudo-genes in the mitochondrial genome of the velvet worm *Metaperipatus inae* (Onychophora, Peripatopsidae). Mol Phylogenet Evol 57:293–300.

Campbell LI, Rota-Stabelli O, Edgecombe GD, Marchioroc T, Longhorna SJ, Telford MJ, Philippe H, Rebecchi L, Peterson KJ, Pisani D. 2011. MicroRNAs and phylogenomics resolve the relationships of Tardigrada and suggest that velvet worms are the sister group of Arthropoda. Proc Natl Acad Sci USA 108:15920–4.

Campiglia S, Lavallard R. 1989. Contribution to the biology of *Peripatus acacioi* Marcus and Marcus (Onychophora, Peripatidae). IV. On the ecdysis at birth. Vie Milieu 39:49–55.

Campiglia S, Lavallard R. 1990. On the ecdysis at birth and intermoult period of gravid and young *Peripatus acacioi* (Onychophora, Peripatidae). In: Minelli A, editor. Proceedings of the 7th Internnational Congress Myriapodology. Leiden, New York: E.J. Brill. p. 461.

Cribb BW, Rathmell A, Charters R, Rasch R, Huang H, Tibbetts IR. 2009. Structure, composition and properties of naturally occurring non-calcified crustacean cuticle. Arthropod Struct Dev 38:173–8.

de Mets R, Nayak NA, Gregoire C. 1964. On submicroscopic structure of the peritrophic membrane and of some excreta of *Peripatus trinidadensis* (Onychophora). Proc Natl Inst Sci India Part B 30:131–5.

Eriksson BJ, Budd GE. 2000. Onychophoran cephalic nerves and their bearing on our understanding of head segmentation and stem-group evolution of Arthropoda. Arthropod Struct Dev 29:197–209.

Eriksson BJ, Tait NN, Budd GE. 2003. Head development in the onychophoran *Euperipatoides kanangrensis*. With particular reference to the central nervous system. J Morphol 255:1–23.

Eriksson BJ, Tait NN, Budd GE, Janssen R, Akam M. 2010. Head patterning and Hox gene expression in an onychophoran and its implications for the arthropod head problem. Dev Genes Evol 220:117–22.

Greving I, Wilde F, Ogurreck M, Herzen J, Hammel JU, Hipp A, Friedrich F, Lottermoser L, Dose T, Burmester H, et al. P05 imaging beamline at PETRA III: first results. In: Stuart RS, editor. Proceedings of the SPIE 9212, Developments in X-Ray Tomography IX, 92120O, August 17, 2014; San Diego, CA, USA. p. 1–8.

Guidetti R, Altiero T, Marchioro T, Sarzi Amadé LS, Avdonina AM, Bertolani R, Rebecchi L. 2012. Form and function of the feeding apparatus in Eutardigrada (Tardigrada). Zoomorphology 131:127–48.

Hackman RH, Goldberg M. 1975. Peripatus: its affinities and its cuticle. Science 190:582–3.

Haibel A, Beckmann F, Dose T, Herzen J, Ogurreck M, Müller M, Schreyer A. 2010. Latest developments in micro-tomography and nanotomography at PETRA III. Powder Diffrac 25:161–4.

Halberg KA, Persson D, Møbjerg N, Wanninger A, Kristensen RM. 2009. Myoanatomy of the marine tardigrade *Halobiotus crispae* (Eutardigrada: Hypsibiidae). J Morphol 270:996–1013.

Haug JT, Mayer G, Haug C, Briggs DEG. 2012. A Carboniferous non-onychophoran lobopodian reveals long-term survival of a Cambrian morphotype. Curr Biol 22:1673–5.

Henry LM. 1948. The nervous system and the segmentation of the head in the Annulata. Microentomology 13:27–48.

Hoffmann KH. 1997. Ecdysteroids in adult females of a ''walking worm'': *Euperipatoides leuckartii* (Onychophora, Peripatopsidae). Invertebr Reprod Dev 32:27–30.

Holliday RA. 1942. Some observations on Natal Onychophora. Ann Natal Mus 10:237–44.

Hou XG, Bergström J. 1995. Cambrian lobopodians—ancestors of extant onychophorans? Zool J Linn Soc 114:3–19.

Hou XG, Ma XY, Zhao J, Bergström J. 2004. The lobopodian *Paucipodia inermis* from the Lower Cambrian Chengjiang fauna, Yunnan, China. Lethaia 37:235–44.

Huesman RH, Gullberg GT, Greenbeg WL, Budinger TF. 1977. RECLBL library users manual—donner algorithms for reconstruction tomography. Berkeley, USA: Lawrence Berkeley Laboratory, University of California.

Kennel J. 1885. Entwicklungsgeschichte von *Peripatus edwardsii* Blanch. und *Peripatus torquatus* n.sp. I. Theil. Arbeiten aus dem Zoologisch-Zootomischen Institut in Würzburg 7:95–229.

Krishnan G. 1970. Chemical nature of the cuticle and its mode of hardening in *Eoperipatus weldoni*. Acta Histochem 37:1–17.

Lavallard R, Campiglia S. 1971. Données cytochimiques et ultrastructurales sur les tubes sécréteurs des glandes de la glu chez *Peripatus acacioi* Marcus et Marcus (Onychophore). Zeitschrift für Zellforschung und mikroskopische Anatomie 118:12–34.

Liu J, Dunlop JA. 2014. Cambrian lobopodians: a review of recent progress in our understanding of their morphology and evolution. Palaeogeogr Palaeoclimatol Palaeoecol 398:4–15.

Liu J, Steiner M, Dunlop JA, Keupp H, Shu D, Ou Q, Han J, Zhang Z, Zhang X. 2011. An armoured Cambrian lobopodian from China with arthropod-like appendages. Nature 470:526–30.

Lotmar W, Picken LER. 1950. A new crystallographic modification of chitin and its distribution. Experientia 6:58–9.

Ma X, Hou X, Bergström J. 2009. Morphology of *Luolishania longicruris* (Lower Cambrian, Chengjiang Lagerstätte, SW China) and the phylogenetic relationships within lobopodians. Arthropod Struct Dev 38:271–91.

Maas A, Mayer G, Kristensen RM, Waloszek D. 2007. A Cambrian micro-lobopodian and the evolution of arthropod locomotion and reproduction. Chin Sci Bull 52:3385–92.

Manton SM. 1938. Studies on the Onychophora—VI. The life-history of *Peripatopsis*. Ann Mag Nat Hist 1:515–29.

Manton SM, Heatley NG. 1937. Studies on the Onychophora. II. The feeding, digestion, excretion, and food storage of *Peripatopsis*, with biochemical estimations and analyses. Phil Trans R Soc B Biol Sci 227:411–64.

Martin C, Mayer G. 2014. Neuronal tracing of oral nerves in a velvet worm—implications for the evolution of the ecdysozoan brain. Front Neuroanat 7:1–13.

Mayer G. 2006. Origin and differentiation of nephridia in the Onychophora provide no support for the Articulata. Zoomorphology 125:1–12.

Mayer G. 2007. *Metaperipatus inae* sp. nov. (Onychophora: Peripatopsidae) from Chile with a novel ovarian type and dermal insemination. Zootaxa 1440:21–37.

Mayer G. Forthcoming 2015. Onychophora. In: Schmidt-Rhaesa A, Harzsch S, Purschke G, editors. Structure and evolution of invertebrate nervous systems. Oxford: Oxford University Press.

Mayer G, Bartolomaeus T, Ruhberg H. 2005. Ultrastructure of mesoderm in embryos of *Opisthopatus roseus* (Onychophora, Peripatopsidae): revision of the ''Long Germ Band'' hypothesis for *Opisthopatus*. J Morphol 263:60–70.

Mayer G, Kauschke S, Rüdiger J, Stevenson PA. 2013a. Neural markers reveal a one-segmented head in tardigrades (water bears). PLoS One 8:e59090.

Mayer G, Martin C, Rüdiger J, Kauschke S, Stevenson PA, Poprawa I, Hohberg K, Schill RO, Pflüger H-J, Schlegel M. 2013b. Selective neuronal staining in tardigrades and onychophorans provides insights into the evolution of segmental ganglia in panarthropods. BMC Evol Biol 13:230.

Mayer G, Oliveira IS. 2013. Phylum Onychophora Grube, 1853. In: Zhang Z-Q, editor. Animal biodiversity: an outline of higher-level classification and survey of taxonomic richness (Addenda 2013). Zootaxa 3703:15–6.

Mayer G, Tait NN. 2009. Position and development of oocytes in velvet worms shed light on the evolution of the ovary in Onychophora and Arthropoda. Zool J Linn Soc 157:17–33.

Mayer G, Whitington PM. 2009a. Neural development in Onychophora (velvet worms) suggests a step-wise evolution of segmentation in the nervous system of Panarthropoda. Dev Biol 335:263–75.

Mayer G, Whitington PM. 2009b. Velvet worm development links myriapods with chelicerates. Proc R Soc B Biol Sci 276:3571–9.

Mayer G, Whitington PM, Sunnucks P, Pfluüger H-J. 2010. A revision of brain composition in Onychophora (velvet

worms) suggests that the tritocerebrum evolved in arthropods. BMC Evol Biol 10:255.
Murdock DJE, Gabbott SE, Mayer G, Purnell MA. 2014. Decay of velvet worms (Onychophora), and bias in the fossil record of lobopodians. BMC Evol Biol 14:222.
Murienne J, Daniels SR, Buckley TR, Mayer G, Giribet G. 2014. A living fossil tale of Pangean biogeography. Proc R Soc B Biol Sci 281:1471–2954.
Nielsen C. 2012. Animal evolution: interrelationships of the living phyla. Oxford: Oxford University Press.
Nielsen C. 2013. The triradiate sucking pharynx in animal phylogeny. Invertebr Biol 132:1–13.
Oliveira IS, Franke FA, Hering L, Schaffer S, Rowell DM, Weck-Heimann A, Monge-Nájera J, Morera-Brenes B, Mayer G. 2012a. Unexplored character diversity in Onychophora (velvet worms): a comparative study of three peripatid species. PLoS One 7:e51220.
Oliveira IS, Lacorte GA, Fonseca CG, Wieloch AH, Mayer G. 2011. Cryptic speciation in Brazilian *Epiperipatus* (Onychophora: Peripatidae) reveals an underestimated diversity among the peripatid velvet worms. PLoS One 6:e19973.
Oliveira IS, Mayer G. 2013. Apodemes associated with limbs support serial homology of claws and jaws in Onychophora (velvet worms). J Morphol 274:1180–90.
Oliveira IS, Read VMSJ, Mayer G. 2012b. A world checklist of Onychophora (velvet worms), with notes on nomenclature and status of names. ZooKeys 211:1–70.
Oliveira IS, Wieloch AH, Mayer G. 2010. Revised taxonomy and redescription of two species of the Peripatidae (Onychophora) from Brazil: a step towards consistent terminology of morphological characters. Zootaxa 2493:16–34.
Ou Q, Shu D, Mayer G. 2012. Cambrian lobopodians and extant onychophorans provide new insights into early cephalization in Panarthropoda. Nat Commun 3:1261.
Read VMSJ, Hughes RN. 1987. Feeding behaviour and prey choice in *Macroperipatus torquatus* (Onychophora). Proc R Soc Lond B Biol Sci 230:483–506.
Reinhard J, Rowell DM. 2005. Social behaviour in an Australian velvet worm, *Euperipatoides rowelli* (Onychophora: Peripatopsidae). J Zool 267:1–7.
Rota-Stabelli O, Kayal E, Gleeson D, Daub J, Boore J, Telford M, Pisani D, Blaxter M, Lavrov D. 2010. Ecdysozoan mitogenomics: evidence for a common origin of the legged invertebrates, the Panarthropoda. Genome Biol Evol 2:425–40.
Rudall KM. 1955. The distribution of collagen and chitin. Symp Soc Exp Biol 9:49–70.
Ruhberg H. 1985. Die Peripatopsidae (Onychophora). Systematik, Ökologie, Chorologie und phylogenetische Aspekte. In: Schaller F, editor. Zoologica, Heft 137. Stuttgart: E. Schweizerbart'sche Verlagsbuchhandlung. p. 1–183.
Ruhberg H, Mayer G. 2013. Onychophora, Stummelfüßer. In: Westheide W, Rieger G, editors. Spezielle Zoologie. Teil 1. Einzeller und Wirbellose Tiere. Berlin: Springer-Verlag. p. 457–64.
Ruhberg H, Storch V. 1977. Über Wehrdrüsen und Wehrsekret von *Peripatopsis moseleyi* (Onychophora). Zoologischer Anzeiger 198:9–19.
Schindelin J, Arganda-Carreras I, Frise E, Kaynig V, Longair M, Pietzsch T, Preibisch S, Rueden C, Saalfeld S, Schmid B, et al. 2012. Fiji: an open-source platform for biological-image analysis. Nat Methods 9:676–82.
Schofield RM, Nesson MH, Richardson KA, Wyeth P. 2003. Zinc is incorporated into cuticular ''tools'' after ecdysis: the time course of the zinc distribution in ''tools'' and whole bodies of an ant and a scorpion. J Insect Physiol 49:31–44.
Sevier CS, Kaiser CA. 2002. Formation and transfer of disulphide bonds in living cells. Nat Rev Mol Cell Biol 3:836–47.
Smith MR, Ortega-Hernández J. 2014. *Hallucigenia*'s onychophoran-like claws and the case for Tactopoda. Nature 514:363–6.
Subramoniam T, Azariah J. 1974. On the structure and histochemistry of the cuticle of austroperipatus *Peripatoides novae zealandiae*. Acta Histochem 50:75–83.
Whitington PM, Mayer G. 2011. The origins of the arthropod nervous system: insights from the Onychophora. Arthropod Struct Dev 40:193–209.